

Large-Eddy Simulations of Baroclinic Instability and Turbulent Mixing

Eric D. Skillingstad
College of Oceanic and Atmospheric Sciences
Oregon State University
104 COAS Admin. Bldg.
Corvallis, OR 97331

Phone: (541) 737-5697 Fax: (541) 737-2064 Email: skylling@coas.oregonstate.edu

Roger M. Samelson
College of Oceanic and Atmospheric Sciences
Oregon State University
104 COAS Admin. Bldg.
Corvallis, OR 97331

Phone: (541) 737-4752 Fax: (541) 737-2064 Email: rsamelson@coas.oregonstate.edu

Award Number: N00014-09-1-0268

LONG-TERM GOAL

The long-term goal of this project is to improve our ability to understand, model and predict lateral mixing and the associated submesoscale physical structure and processes in the upper and interior ocean.

OBJECTIVES

The main objective of this project is to examine the interaction between baroclinic, mesoscale eddies and turbulence using a large-eddy simulation (LES) model. Cases will focus on strong, baroclinic waves that form in the mixed layer along surface fronts with scales of a few km, and on mesoscale eddies that are imbedded within larger scale frontal regions. Our goal is to quantify, understand, and ultimately parameterize the physical processes that lead to lateral mixing. Simulations will help guide field experiments planned as part of the Lateral Mixing DRI, and provide a tool for understanding observations in the analysis phase of the project.

APPROACH

High-resolution simulations of baroclinic instability and the interaction of mesoscale flow with turbulent mixing are conducted and analyzed using a large-eddy simulation model. Our analysis centers on quantifying and understanding the mechanisms by which small-scale turbulent structure develops on the mesoscale field, the physical processes and balances that control lateral mixing of fluid properties across the unstable front, and the transition from strongly horizontal, geostrophic motion on the mesoscale to three-dimensional, quasi-isotropic, non-hydrostatic motion on turbulent scales.

WORK COMPLETED

Research during the fourth year of this project has focused on extending the analysis of baroclinic instability and performing a mixed layer experiment to examine dye dispersion.

RESULTS

Baroclinic Wave Experiments

Novel numerical simulations of baroclinic instability of a shallow, geostrophically balanced, density filament were reported that resolved the full range of motions from rotationally dominated, growing baroclinic waves (Figure 1) to quasi-isotropic, three-dimensional shear instabilities (Figure 2).

The simulations (Figures 1-4) demonstrate that shear generated in narrow frontal zones can support weak three-dimensional turbulence that is directly linked to the larger-scale baroclinic waves. Two separate but closely related issues are addressed: (1) the possible development of enhanced turbulent mixing associated with the baroclinic wave activity, and (2) the existence of a downscale transfer of energy from the baroclinic wave scale to the turbulent dissipation scale. The simulations show enhanced turbulence (Figures 2,3) associated with the baroclinic waves (Figure 1), and enhanced turbulent heat flux across the isotherms of the imposed frontal boundary, relative to background levels (Figure 4). This turbulence develops on isolated small-scale frontal features that form as the result of frontogenetic processes operating on the baroclinic wave scale (Figure 1), and not as the result of a continuous, inertial forward cascade through the intermediate scales. Analysis of the spectrally decomposed kinetic energy budget indicates that large-scale baroclinic eddy energy is directly transferred to small-scale turbulence, with weaker forcing at intermediate scales. The results confirm a forty-year-old prediction (Hoskins and Bretherton, 1972) that frontogenesis driven by baroclinic-wave deformation fields will cause a collapse of cross-frontal spatial scales that will continue to the Kelvin-Helmholtz turbulent transition. The simulations isolate and illustrate a mechanism for spontaneous loss of balance in an initially geostrophic flow, and a direct, spectrally non-local pathway for downscale energy transfer that is phenomenologically distinct from traditional concepts of turbulent cascades.

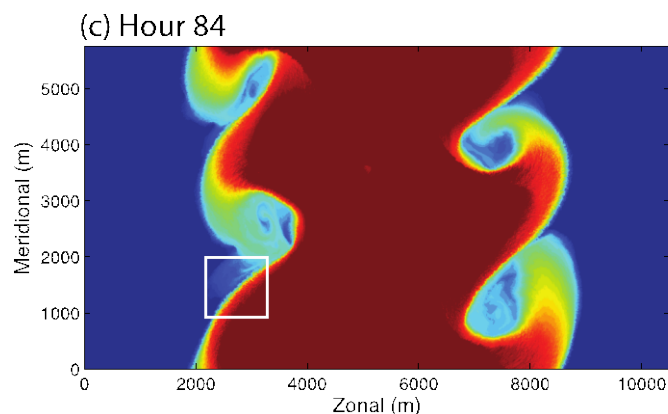


Figure 1: *The surface temperature field at hour 84 shows the development of baroclinic waves with along-front wavelength of roughly 3 km. In areas of baroclinic surface convergence (such as the region denoted by the white box), frontogenesis occurs, with intensification of the surface temperature gradients and the associated alongfront geostrophic velocities and thermal wind vertical shear. This results in a local reduction of the bulk Richardson number below critical values for turbulent transition.*

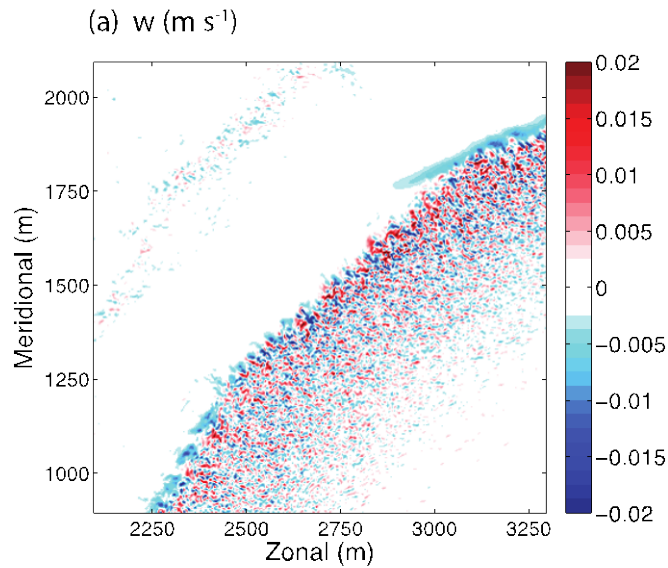


Figure 2: At hour 84, the vertical (pictured, for the region enclosed by the white box in Figure 1) and horizontal (not shown) velocity fields have developed energetic small-scale structure along the intensified surface front. This structure, which is resolved by the isotropic 3-m finite-difference grid, is the signature of Kelvin-Helmholtz turbulent transitions associated with the intensified vertical shear in the frontogenetic zone.

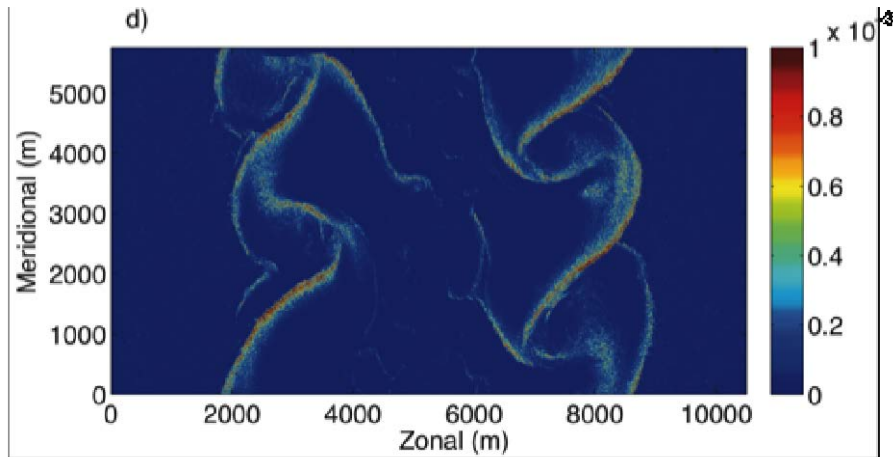


Figure 3: At hour 84, the near-surface turbulent eddy thermal diffusivity across the full domain shows systematic intensification by an order of magnitude or more in the frontogenetic zones. This intensification is the result of the energetic small-scale turbulent motions (Figure 2) that develop from the intensified vertical shear.

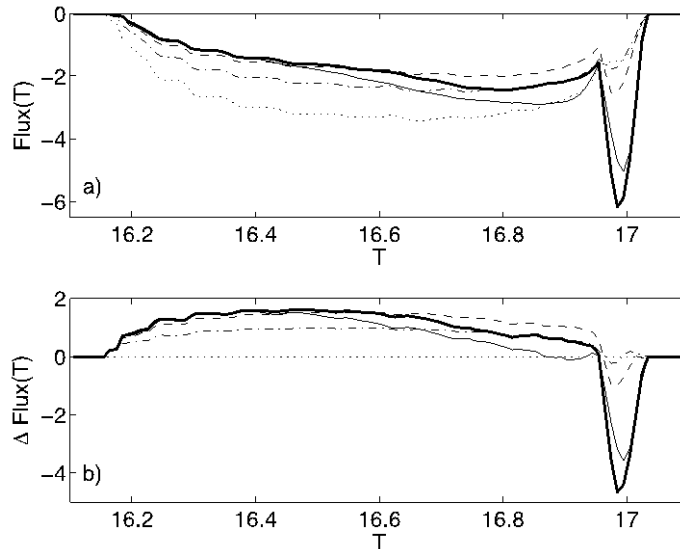


Figure 4. *The enhanced turbulent diffusivities in the frontogenetic zones (Figure 3) cause enhanced internal turbulent heat fluxes across frontal isothermal surfaces. (a) Area-integrated sub-grid-scale turbulent diffusive heat (“temperature”) fluxes H_T ($^{\circ}\text{C m}^3 \text{s}^{-1}$) through the frontal isothermal surfaces $16.1^{\circ}\text{C} < T < 17.1^{\circ}\text{C}$ at hours 48 (dotted), 60 (dashed-dotted), 72 (dashed), 84 (thick solid), 96 (thin solid). (b) Differences of corresponding fluxes from hour-48 values.*

Additional details are available in Skillingstad and Samelson (2012), with extensions reported also by Samelson and Skillingstad (2012).

Mixed Layer Experiments

Mixed layer simulations are conducted using the three-dimensional ocean large-eddy simulation model with added surface wave effects (Skillingstad et al. 2000) and two different initial conditions. The first initialization simulates the behavior of a warm filament with two fronts; the second initialization applies uniform conditions with a fixed horizontal temperature gradient. Both cases are forced with a northerly wind stress of 0.1 N m^{-2} and in surface wave cases, Stokes drift for a 30-m wavelength surface wave with 1.0 m amplitude. The ocean mixed layer depth and frontal strength in these experiments was chosen to roughly match conditions that were observed on June 16, 2011 during the Latmix I surface dye release experiment.

Our first simulation focused on the effects of down front winds on a finite width front as represented by the warm filament initialization (Figure 5). At first, linear disturbances aligned along the front suggest that symmetric instability is active in the down front wind case. However, the symmetric orientation is short lived and the structures soon rotate away from the wind, eventually forming an angle of about 30-45 degrees to the frontal axis. Larger scale baroclinic waves appear to be suppressed with the front fracturing into chaotic eddy motions over time.

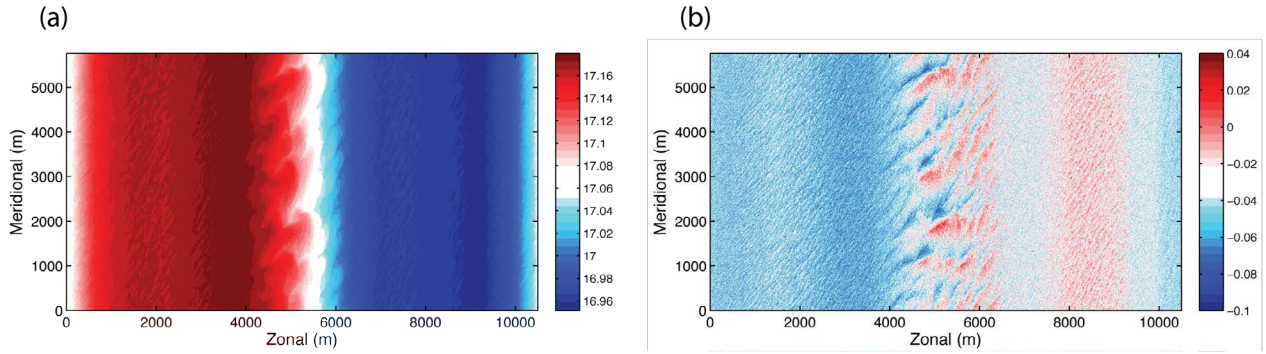


Figure 5. Warm filament simulation (a) temperature and (b) u velocity component (m/s), at hour 24, for northerly wind and surface wave forcing. Coherent structures aligned 30-45 degrees from the frontal (meridional, y) axis are visible for $4000\text{ m} < x < 6000\text{ m}$.

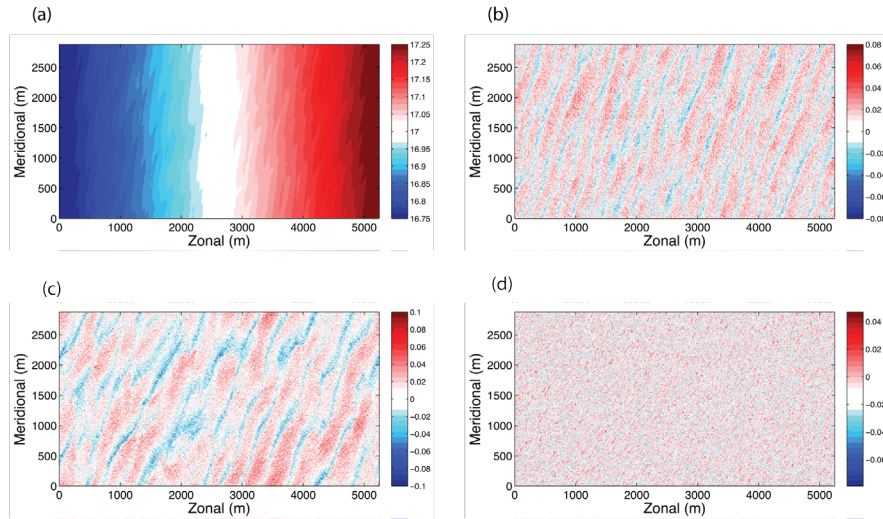


Figure 6. Constant gradient simulation plots of (a) temperature and (b) u component velocity (m/s) at hour 24 with Stokes drift forcing, (c) u component velocity (m/s) without Stokes drift, and (d) u component (m/s) for a case with Stokes drift but no constant gradient.

The warm filament experiment raised a number of questions, for example, what process generates the coherent velocity structures and how important are these structures dependent on a finite-width front? To explore these questions, we conducted a second simulation using a uniform geostrophic balanced horizontal density gradient, similar to that of Taylor and Ferrari (2010) but in a rectangular domain similar to the two-front case. Results from this case (Figure 6), like the two-front simulation, show the generation of coherent structures that form at a ~ 30 degree angle to the front, but now extending across the entire domain. These structures did not form in a simulation with the same surface forcing, but with no horizontal gradient and geostrophic flow (Fig. 6d). Also shown in figure 6c is a case with surface wave effects removed from the forcing, showing that Langmuir circulation is not critical for these coherent circulations, but does have an effect on the cell spacing.

We conclude from these experiments that the existence of the frontal-zone horizontal temperature gradients and the associated geostrophic currents are essential to the coherent roll structures in the turbulent ocean boundary layer, but that the isolated character of the gradient regions in the two-front case is not essential to the formation of these structures.

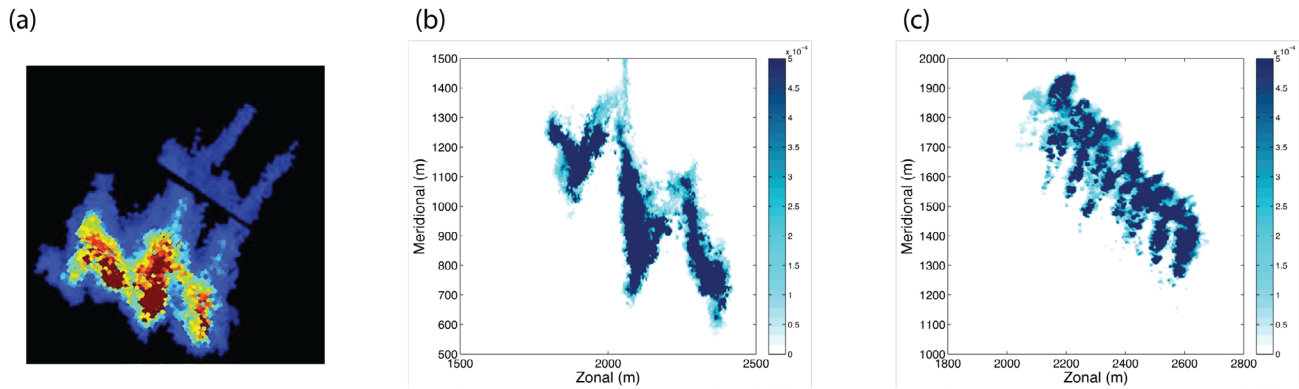


Figure 7. Plots of (a) Lidar return signal from dye released in a 20 m deep mixed layer after 2 hours, (b) simulated dye concentration at a depth of 18 m with constant horizontal temperature gradient, (c) simulated dye concentration without a constant density gradient. The Lidar image size is approximately 800 m x 800 m.

Dye patterns observed during the Latmix I mixed layer experiment clearly show coherent structures with horizontal scales many times the mixed layer depth. To examine how dye behaves using the model, we initialized a 500 m long tracer patch at hour 1 of the simulation and allowed the tracer to advect and diffuse in the model as a passive tracer. Simulated dye concentration after 1.9 hours of transport and diffusion for the constant gradient case (Figure 7) shows structures with scales close to the observed dye patch. In contrast, dye in the homogeneous case (Figure 7c) indicates much smaller structures. Simulations also indicate that the circulations transport dye into the upper pycnocline, similar to the observed dye patch measured by the airborne Lidar.

Further research is needed to better understand the processes active in forming frontal zone mixed layer instabilities. Because the circulations do not display strong symmetry across the front, it is unlikely that strict symmetric instability theory applies in this case. An alternative explanation might be boundary layer roll instabilities as studied in the atmosphere by Lilly (1966). However, Lilly's development does not depend on a front but only requires a constant background geostrophic flow. Modification of the Lilly theory with geostrophic shear could prove effective in understanding these structures.

REFERENCES

- Lilly, Douglas K., 1966: On the Instability of Ekman Boundary Flow. *J. Atmos. Sci.*, **23**, 481–494.
- Samelson, R. M., and E. D. Skillingstad, 2012. Pipelining the cascade: Kelvin-Helmholtz transitions in simulations of baroclinic waves. AGU Fall Meeting. [abstract only]
- Skillingstad, E.D., W.D. Smyth, and G.B. Crawford, 2000. Resonant wind-driven mixing in the ocean boundary layer. *J. Phys. Oceanogr.*, **30**, 1866-1890.

Taylor, J. R., and R. Ferrari, 2010: Buoyancy and wind-driven convection at mixed layer density fronts. *J. Phys. Oceanogr.*, 40, 1222-1242

PUBLICATIONS

Skyllingstad, E. D. and R. M. Samelson, 2012. Baroclinic Frontal Instabilities and Turbulent Mixing in the Surface Boundary Layer. Part I: Unforced, *J. Phys. Oceanogr.*, 1701-1716.